Uncertainties in observations and climate projections for the North East India

Bidyabati Soraisam[a,*], Ashok Karumuri[a], Pai D.S.[b]

[a] University Centre for Earth, Ocean and Atmospheric Sciences, University of Hyderabad, Gachibowli, Hyderabad, Telangana 500046, India
[b] India Meteorological Department, Pune 411 005, India

ARTICLE INFO

ABSTRACT

The Northeast-India has undergone many changes in climatic-vegetation related issues in the last few decades due to increased human activities. However, lack of observations makes it difficult to ascertain the climate change. The study involves the mean, seasonal cycle, trend and extreme-month analysis for summer-monsoon and winter seasons of observed climate data from Indian Meteorological Department ($1° \times 1°$) and Aphrodite & CRU-reanalysis (both $0.5° \times 0.5°$), and five regional-climate-model simulations (LMDZ, MPI, GFDL, CNRM and ACCESS) data from AR5/CORDEX-South-Asia ($0.5° \times 0.5°$). Long-term (1970–2005) observed, minimum and maximum monthly temperature and precipitation, and the corresponding CORDEX-South-Asia data for historical (1970–2005) and future-projections of RCP4.5 (2011–2060) have been analyzed for long-term trends. A large spread is found across the models in spatial distributions of various mean maximum/minimum climate statistics, though models capture a similar trend in the corresponding area-averaged seasonal cycles qualitatively. Our observational analysis broadly suggests that there is no significant trend in rainfall. Significant trends are observed in the area-averaged minimum temperature during winter. All the CORDEX-South-Asia simulations for the future project either a decreasing insignificant trend in seasonal precipitation, but increasing trend for both seasonal maximum and minimum temperature over the northeast India. The frequency of extreme monthly maximum and minimum temperature are projected to increase. It is not clear from future projections how the extreme rainfall months during JJAS may change. The results show the uncertainty exists in the CORDEX-South-Asia model projections over the region in spite of the relatively high resolution.

1. Introduction

The WG1 (Working Group I) report of the IPCC (2013) states that global warming occurring since 1950's is unequivocal and unprecedented over decades to millennia, and that human influence has been detected in the warming of the atmosphere and oceans. CMIP5 (Coupled model intercomparison project phase 5) models simulation have also projected an increase in global mean surface temperature over a range from 1.1 °C to 2.6 °C (IPCC, 2013), which seems to be qualitatively realistic as seen from the consistently increasing global temperatures.

Anthropogenic climate change manifested in changing temperature and precipitation, and is likely to pose serious risk to human society, economy and ecosystems, such as loss of agriculture, water shortages and widespread health impacts as well as increased in heat-induced mortality to extreme events, etc. (Kumar et al., 2006; Kumar et al., 2011; Ravindranath et al., 2011; Jain et al., 2012; Choudhury et al., 2012 and Sharmila et al., 2015). The effects of climate change are expected to be greatest in the developing countries which rely on primary production as a major source of income (Kumar et al., 2006). According to the Fourth and Fifth Assessment Reports of the Intergovernmental Panel on Climate Change (IPCC, 2007 and 2013), the Indian subcontinent will be adversely affected by enhanced variability of climate, rising temperature and substantial changes summer rainfall in some parts and thereby water stress by the 2020s.

Several studies from the CMIP3 and CMIP5 simulations (Kumar et al., 2006; Chaturvedi et al., 2012; Kumar et al., 2013; Dufresne et al., 2013 and Jourdain et al., 2013, etc.) and several studies based on the downscaled projections (Kumar et al., 2011; Dash et al., 2012; Kumar et al., 2013 and Krishnan et al., 2016) project an increasing trend in the atmospheric temperature over India associated with increased anthropogenic activities. This conjecture also matches with the results from observational studies such as those by Kothawale et al. (2012) and Kothawale and Kumar (2005) and Revadekar et al. (2012) which show an increase of surface temperatures across various regions of India during the recent 3–4 decades as compared to the earlier period.

Notwithstanding this, the CMIP3 models as well as those from the CMIP5 (Collins et al., 2013; Dufresne et al., 2013; Jourdain et al., 2013; Saha et al., 2014 and Sharmila et al., 2015) have challenges in simulating the teleconnections and trends of the Indian summer monsoon rainfall, which is seasonally phaselocked to the June–September months (henceforth JJAS), correctly. Though the CMIP5 models show better skills in reproducing the mean Indian summer monsoon rainfall (Jourdain et al., 2013 and Shashikanth et al., 2013), the amplitude of interannual variability and seasonal cycle reasonably close to the observations data as compared to the best CMIP3 models (Jourdain et al., 2013). The decreasing Indian summer monsoon rainfall trend during the past decades (Guhathakurta and Rajeevan, 2008; Rajendran et al., 2013 and Krishnan et al., 2016, etc.) is not reproduced by the CMIP5 models, which is a serious limitation of the GCMs at coarse resolution in capturing the south Asian climate change in the recent decades (Krishnan et al., 2016 and Roxy et al., 2015).

Fortunately, dynamical downscaling of the historical simulations by various regional climate models (Dash and Hunt, 2007; Dash et al., 2012, Dash et al., 2015) or using high resolution GCMs in the Indian region (Krishnan et al., 2016) have been successful in capturing the decreasing Indian Summer Monsoon Rainfall trend (ISMR), which is essentially area-averaged June–September rainfall over a major homogeneous rainfall region of India (northeast India not included). Therefore, the corresponding future projection of a weakening ISMR trend by the high resolution models (e.g. Dash et al., 2015; Krishnan et al., 2016) may have some reliability in a qualitative sense. Some of these studies are sort of a first but sure step in understanding the relative contribution of various climate change drivers such as greenhouse gases, aerosols, and land surface processes (Kothawale et al., 2012; Krishnan et al., 2016 and Roxy et al., 2015). Having said that, if sub-regional level in India is concerned, uncertainties exist in some climate statistics across various observational datasets, and high resolution projections as well (Kumar et al., 2013).

The northeast India (NEI) is a prominent portion of India, covering a geographic area of 26.2 mha, and home to a population of about 45 million (Ministry of Home Affairs, Government of India). In India, the characteristics of the summer monsoon rainfall and its variability differ from region to region within the nation (Mooley and Parthasarathy, 1983a, 1983b). An empirical orthogonal analysis by Parthasarathy et al. (1996) of long term summer monsoon rainfall records for the 1871–1990 from 306 stations widely-distributed stations in India shows a dipolar structure of the gravest mode, wherein the signal in the northeast India is seen in an out of phase relation with the rest of India (see Fig. 6.5, Pant and Kumar, 1997). The NEI is also endemic to many flora and fauna making it one of the richest in the world in terms of biological values (Chakraborty et al., 2012). It has a subtropical climate with wide variation in weather and climate, and is characterized by large rural population (82%), low population density, large percentage of indigenous tribal communities (34–91%) and large area under forests (60%) (Ravindranath et al., 2011). The NEI is highly dependent on the south west monsoon and over 60% of the crop area is under rain-fed agriculture (Ravindranath et al., 2011). However, the climate statistics vary from study to study owing to the rather sparse observations and computational methods that depend on the area over which the rainfall is averaged, and the method of averaging. For example, Parthasarathy et al. (1996) compute the summer monsoon rainfall over the homogeneous Northeast Indian region to be 142 cm. Nonetheless, it is clear that the region receives a high seasonal rainfall during JJAS.

Dash et al. (2015) analyzed temporal trends in rainfall from nine stations in the NEI on monthly, seasonal and annual scales for 1961–2010. Several other studies that analyze station data from about 7 sub-divisions (Jain et al., 2012), 9 stations (Laskar et al., 2014) and 2 sub-divisions (Mondal et al., 2014) in NEI over the period of 1913–2012, or part of this period, also support this finding of Dash et al. (2015).

On the temperature front, (Jain et al., 2012; Laskar et al., 2014; Mondal et al., 2014, and Wagholikar et al., 2014) have analyzed either the temperature recorded at a few station in the NEI or the homogenized regional temperature records for the 1871–2008, or a portion of that period. These studies suggest an increasing trend in the maximum and/or minimum temperature in some portions of the NEI. Mondal et al. (2014) states that the NEI region is clearly seen affecting by climate change which may lead to droughts in the future due to decrease in rainfall and increase in temperature. Arora et al. (2005) evaluated the temperature trends based on 125 stations in NEI which showed a falling trend in annual mean minimum temperature as most of the stations are located in the foothills of the Himalayas. Climate change vulnerability profiles have been developed at the district level in NEI for agriculture, water and forest sectors for the current and projected future climates where the majority of the districts are subjected to climate induced vulnerability currently and in the near future (Ravindranath et al., 2011). These studies, in general hint, show a significant rise in the observed temperature, and a decreasing tendency in rainfall in various places in the northeast India.

As far as the model studies are concerned, so far, only Dash et al. (2012) have studied the recent and projected future changes in precipitation and temperature of the NEI by downscaling CMIP3 datasets using RegCM3, for the periods 1971 to 2005, and 2011 to 2100. Dash et al. (2012) also record an overestimation of simulated rainfall by the CMIP3 for 1971–2005, and project an increase in the annual mean temperature by about 0.64 °C from 2011 to 2040, and also an increase in annual mean precipitation by about 0.09 mm/day in the near future and by 0.48 mm/day at the end of the century in NEI. Having said this, it indicates the very limited sample of future climate projections for the northeast Indian climate, which means that there would be a significant uncertainty. The differences in datasets add to the uncertainty associated with the inter-model differences when one tries to validate a climate model simulation, particularly the climate change projections (Jourdain et al., 2013 and Collins et al., 2013). This applies acutely for the NEI (Prakash et al., 2014), where the impact of climate change on NEI is explored lesser both in terms of observational analysis as well as from the modeling perspective (Laskar et al., 2014).

Fortunately, of late, several climate centers have dynamically downscaled various CORDEX South-Asia based on CMIP5 projections for the Indian region. The downscaled simulations-four regional climate models, namely MPI, GFDL, CNRM, ACCESS and a high resolution suite of future climate projections by the LMDZ model (Sabin et al., 2013) are available from the cccr.tropmet.res.in under the aegis of the Co-ordinated Regional Downscaling Experiment, SOUTH ASIA (CORDEX). This gives us an opportunity to address the future climate change in the NEI at a higher resolution, while also taking into account any uncertainty associated with inter-model variability. In addition, we have high resolution gridded rainfall and temperature datasets, derived from the observed IMD datasets among other things, which will be useful to validate the CORDEX South-Asia outputs.

The rest of the current paper is organized as follows. In the next section, we present the study area, various model datasets, and observed and Aphrodite, and reanalyzed climate datasets used, along with a description of our methodology. In the Section 3, we present the results from our analysis, and in the Section 4, our concluding summary and remarks.

2. Datasets and methodology

No study has been done using CORDEX South-Asia output on future scenarios on NEI. Thus the assessment of rainfall and temperature change in the last few decades, and its future projection are very important. These will provide an insight for the present and possible future condition to the planners for climate change adaptation. Taking this note into account, with the help of these five regional climate model data a proper assessment of future trends would help in setting up uncertainties of future for risk management and vulnerability

assessment. Knowledge of spatial and temporal variability of climate parameters is very much useful for overall development of the region and for future planning, which can be attained from this work.

2.1. Model datasets & observational datasets used

In this study, we use the gridded datasets of rainfall (Rajeevan et al., 2005) and temperature (Rajeevan et al., 2008, 2008) derived from the observations the India Meteorological Department (IMD) for the period 1970 to 2005, available at 1° × 1° resolution for temperature and also for precipitation at 1° × 1° resolution. We also use the Asian Precipitation Highly-Resolved Observational Data Integration Towards Evaluation of water resource (Aphrodite) precipitation data with 0.5° × 0.5° resolution from 1970 to 2005 for comparison (Yatagai et al., 2012). For convenience, we refer to these interpolated datasets as 'observations'. Further, as the observations in the NEI are sparse, we also analyze the reanalyzed mean temperature data collected from CRU TS v. 4.00 (0.5° × 0.5° resolution) from 1970 to 2005 (Harris et al., 2014), in addition to the observed temperature datasets from the IMD, in order to have a sense of uncertainty across these two datasets.

In order to estimate the future climate change in the NEI, we also use the high resolution climate model simulation outputs from AR5/CORDEX SOUTH ASIA (See A.1 for details) for the period 1970 to 2005 and 2011 to 2060 at 0.5° × 0.5° resolution. Model-simulated data including maximum and minimum temperature, and precipitation were obtained from the five RCMs[1] that participated in the CORDEX SOUTH ASIA: LMDZ, MPI, GFDL, CNRM and ACCESS. Details on these five model data can be procured from the CCCR, IITM and from the given links, http://cccr.tropmet.res.in/workshop/oct2012/presentations/R%20Krishnan_CCCR_CORDEXSA.pdf http://cccr.tropmet.res.in/workshop/oct2012/presentations/JSanjay_CORDEX-SAsia_RCM_data.pdf http://cordex.dmi.dk/joomla/images/CORDEX/cordex_archive_specifications_120126.pdf Gridded data sets for SST from 1970 to 2005 is collected from HadSST, Met office to see the teleconnections between the precipitation and maximum and minimum temperature datasets with Nino 3.4.

As known, the CORDEX South Asia based on CMIP5 historical runs, forced by observed natural and anthropogenic atmospheric composition, cover the period from 1950 to 2005, whereas the projections from 2011 to 2060 used in the study are forced by Representative Concentration Pathways (RCP) i.e. RCP4.5. As mentioned earlier, we use the downscaled historical simulations of the CORDEX South Asia models for the period 1970–2005 for the NEI, and regional simulations obtained by downscaling RCP4.5 future scenario of the CORDEX South Asia, are used. The CMIP5 historical simulations covers few hundred centuries long pre-industrial and industrial period (from the mid-nineteenth century to near present) control simulations (Taylor et al., 2012 and Dufresne et al., 2013). The CMIP5 RCP4.5 simulations have both natural and anthropogenic forcing, where in the representative concentration pathways have been and were designed to have a top of the atmosphere radiation at 4.5 Wm-2 at the end of 2100 and CO_2 concentration stabilizes at 543 ppmv in 2150. Global CO_2 concentration is directly prescribed in the simulations from 1886 to 2095 for computing radiative budget (Krishnan et al., 2016).

2.2. Model validation

In this paper, the region bounded by the latitudes from 25.5° N through 28.5° N, and longitudes from 92.5° E through 94.5° E is referred to as the northeast India (NEI) for the purpose of statistical analysis such as the area-averaging, etc. The downscaled historical simulations are validated by comparing the mean model climatology with observed

precipitation and temperature patterns. To facilitate this, the observed datasets are resampled into 0.5° resolutions using a bilinear interpolation method. We explore the interannual variability and climate change of the seasonal rainfall and temperature during the two important seasons in the NEI, namely, the monsoon season (JJAS) and the winter season (DJF).

To have an estimate of the future climate change in any climatic parameter C, we subtract the simulated (LMDZ, MPI, GFDL, CNRM and ACCESS) historical climatology of the parameter (precipitation and maximum and minimum temperature), say 'C_{hist}', from the corresponding climatology from the RCP4.5 simulations, say 'C_{RCP}' i.e., $\Delta C = C_{RCP} - C_{hist}$.

In this study, we apply a linear trend analysis, by the method of Least square linear fit (Jhajhariaa and Singh, 2011; Jain and Kumar, 2012 and Dubey and Krishnakumar, 2014), on the simulated and observed data of temperature and precipitation, as necessary. The statistical significance of the identified trend is evaluated using the Mann Kendall (M-K) trend test and Student *t*-test. The M-K test is a non-parametric test for identifying trend in time series data, and extensively used in climate studies in checking spatial variation and temporal deviation of any climatic series (Kumar et al., 2010; Jain and Kumar, 2012; Jain et al., 2012; Laskar et al., 2014 and Chinchorkar et al., 2015). This statistics is used to test the null hypothesis such that no trend exists. The presence of a statistically significant trend is evaluated using the Z value. If the computed value of $|Z| > Z_{\alpha/2}$, the null hypothesis (H_0) is rejected at α level of significance in a two-sided test. A very high positive value of S indicates increasing trend and a very low negative value of S indicates decreasing trend (Laskar et al., 2014). In this study, the M-K test is run at 5% level of significance on time series data. Further details of the M-K test are available in the A.2. Further, the observed and simulated teleconnections with the ENSO have been estimated by using the well-known Nino3.4 index to represent the ENSO activity. The Nino 3.4 index is obtained by area-averaging, the SST anomalies over the 5° N–5° S and 120° W–170° W. We use linear correlation analysis to establish any association of the ENSO events with the NEI climate. Last but not the least, extremes of precipitation and, maximum and minimum temperature of both historical and future projections have been estimated with the help of histogram.

3. Results and discussion

In this section, we study the observed seasonal rainfall and temperature climatologies in the NEI for the 1970–2005 period and the respective long term linear trends therein. We also evaluate the fidelity of the downscaled historical simulations using the observational results. Then we analyze the results from the five downscaled future scenarios, namely, the RCP4.5 simulations (LMDZ, MPI, GFDL, CNRM and ACCESS) available for the period of 2011–2060, in order to decipher the projected climate change in the northeast. The teleconnections of precipitation and, maximum and minimum temperature with the ENSO index known as Nino 3.4 are also studied. And extremes of JJAS and DJF for precipitation, maximum and minimum temperature for both historical and future projections are analyzed in the last part.

3.1. Climatology for JJAS historical simulation from 1970 to 2005

Fig. 1(a) is an effort to validate the simulated, JJAS climatology of precipitation (RF-$_{JJAS}$) for the period of 1970–2005 with that from the IMD observations and the Aphrodite data. We find from spatial distribution of the observed climatological RF-$_{JJAS}$ that it varies from 9 to 22 mm, Aphrodite data ranges from 3 to 13 mm and model data range from 3 to 18 mm. However, as it can be seen that the corresponding climatological RF-$_{JJAS}$ distribution from the Aphrodite datasets as well as those from all models except the LMDZ model show the magnitude of the climatological rainfall increasing from the north towards the south west, and in LMDZ climatology, the RF-$_{JJAS}$ increases towards the south

---

[1] Note that the LMDZ is an atmospheric general circulation model, but with a 0.5° resolution in the Indian region. However, for simplicity, we refer to that as a regional model.
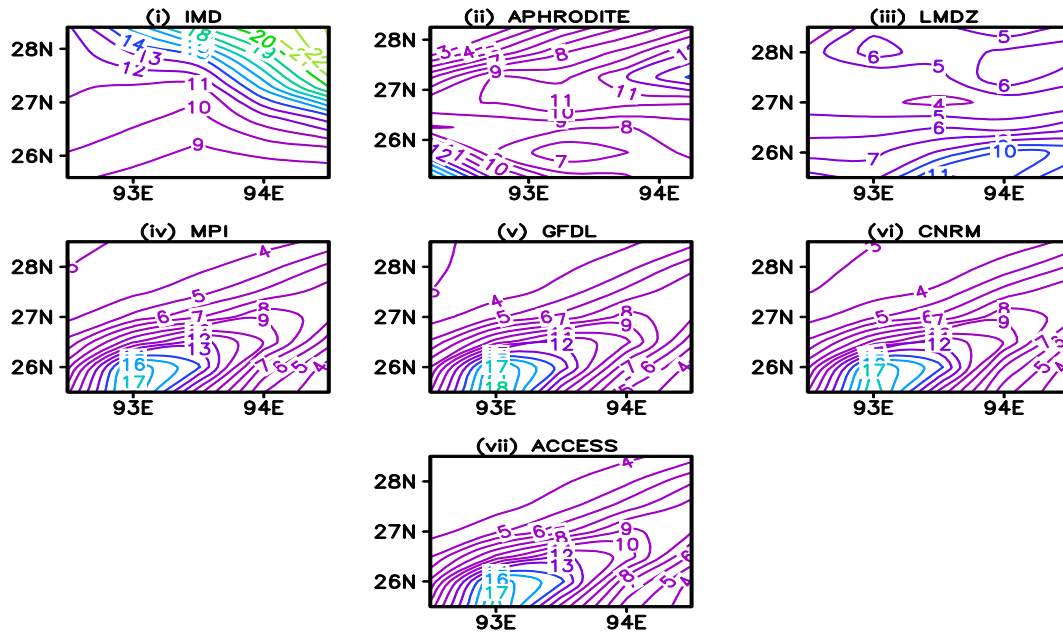
Fig. 1. (a) Spatial distributions of JJAS climatology of precipitation (mm) during 1970–2005 (historical) for (i) IMD, (ii) APHRODITE data, and climate model data from Cordex South Asia: (iii) LMDZ, (iv) MPI, (v) GFDL, (vi) CNRM and (vii) ACCESS over North East Region.

east. Notwithstanding such discrepancy in the gradients, the range of climatological RF-$_{JJAS}$ across the observational datasets as well as models is not much different.

The observed climatological T$_{Max\text{-}JJAS}$ varies from 30.6 °C to 32 °C (Fig. S1, it can be found in supplementary figures and please note that all the figures with S denote the supplementary figures); the maximum T$_{Max\text{-}JJAS}$ occurs approximately in the central north-east, and increases from the west to the east. The spatial distribution of the climatological T$_{Max\text{-}JJAS}$ across the NEI from the CRU reanalysis, ranging from 19 °C to 20.5 °C, decreases in the centre. The CRU data and each model exhibit a relatively broad range of climatologies (T$_{Max\text{-}JJAS}$) across the NEI as compared to the observed data, so the ranges are shown made differently as appropriate. The simulated climatology of the (T$_{Max\text{-}JJAS}$) by various models is lower with different spatial distribution than the observations, with the simulated climatological values varying from 12 °C to 29 °C across the region in models. The LMDZ model shows an increasing T$_{Max\text{-}JJAS}$ from northwest towards the south with the maximum values occur in the centre. The rest of the models show an increasing T$_{Max\text{-}JJAS}$ from northwest towards the south east.

The models also underestimate the climatology of minimum temperature in JJAS (TMin-JJAS) as compared to the CRU reanalysis (Fig. S2), with a simulated range of 3 °C to 22 °C as against the corresponding values of 28 °C to 32 °C in observed data varies from 19 °C to 20.2 °C from the CRU reanalysis datasets.

3.2. Climatology for DJF historical simulation from 1970 to 2005

Fig. S3 shows the DJF climatology of precipitation (RF-$_{DJF}$) for the period 1970–2005, derived from the IMD, Aphrodite and model datasets. The magnitude of the RF-$_{DJF}$ across the NEI ranges between 0.6 and 1.6 mm, with Aphrodite datasets ranging from 0.2 to 0.8 mm and the models, ranging from 0.5 to 3.8 mm, also capturing the relatively low seasonal climatological rainfall during the DJF season (Fig. S3) as compared to the JJAS season (Fig. 1a).

The DJF climatology of maximum temperature (T$_{Max\text{-}DJF}$) in IMD observations varies from 23.4 °C to 24.4 °C (Fig. S4), and increases from the south to north of the NEI. The CRU data ranges from 19 °C to 21.2 °C, with a decrease T$_{Max\text{-}DJF}$ in the centre. The models underestimate the climatological T$_{Max\text{-}DJF}$ in the NEI with the simulated T$_{Max\text{-}}$

$_{DJF}$ ranging from 1 °C to 15 °C.

The simulated winter climatological minimum temperatures (T$_{Min\text{-}DJF}$) in Fig. S5 exhibit a range of values from 10.4 °C to 11 °C, which are relatively nearer to that from the IMD datasets, with CRU data having higher (T$_{Min\text{-}DJF}$).

Table 1 shows the difference in the climatological means of observed data sets from those of the simulated rainfall and, maximum and minimum temperature from 1970 to 2005. In support to the above spatial climatological analysis, the models show a lower means than the observations datasets.

3.3. Seasonal mean cycle for historical simulation from 1970 to 2005

In Fig. 2(a), mean seasonal cycle of precipitation for the 1970 to 2005 from the two observed datasets are shown, along with those from each model. All the datasets show a seasonal evolution similar to observations, with the simulated precipitation from most of the models peaking in July. However, the simulated precipitation from the LMDZ, peaks in the month of August, and the simulated magnitude is in general much less than that from the IMD or Aphrodite datasets. To sum up, the models seem to capture the observed seasonal cycle of mean of precipitation qualitatively for the study region.

The simulated mean seasonal cycles of the maximum and minimum temperatures in the NEI are also qualitatively similar to observations

Table 1
Mean climatological value for observation and model data (1970–2005).

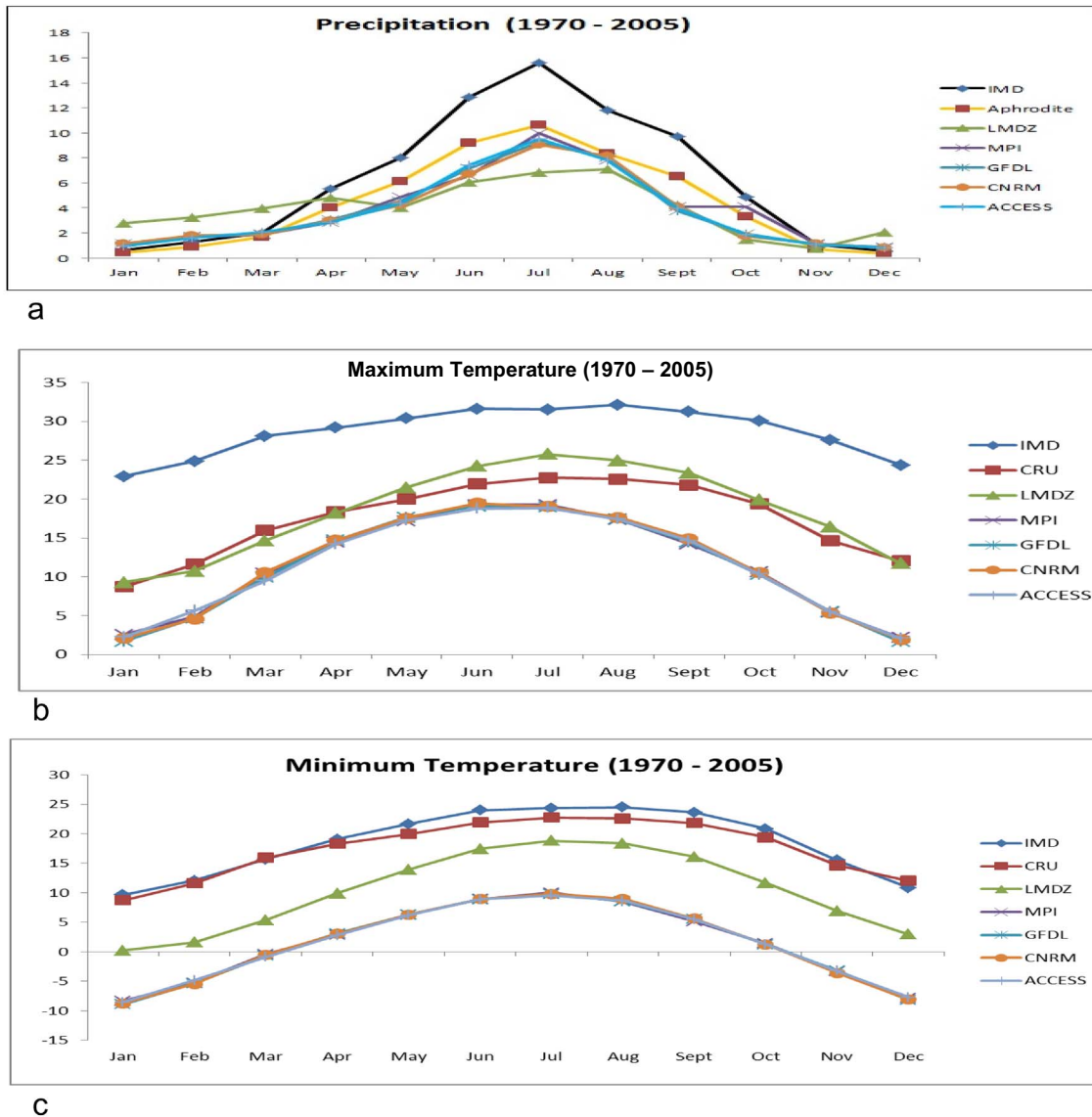| Mean climatology							
	Precipitation			Maximum temperature		Minimum temperature	
	JJAS	DJF		JJAS	DJF	JJAS	DJF
IMD	12.5	0.8	IMD	31.6	24.0	24.1	10.9
APHRODITE	8.7	0.6	CRU	19.6	19.7	19.6	19.7
LMDZ	6.1	2.7	LMDZ	24.6	10.5	17.7	1.6
MPI	7.1	1.2	MPI	17.5	3.2	8.1	−7.1
GFDL	7.0	1.3	GFDL	17.5	2.6	8.2	−7.5
CNRM	6.9	1.3	CNRM	17.7	2.9	8.4	−7.4
ACCESS	7.2	1.1	ACCESS	17.4	3.3	8.1	−6.9

a

b

c

Fig. 2. (a). Seasonal mean cycle of precipitation data (mm) from IMD (observed data), Aphrodite, and Cordex South Asia model data (LMDZ, MPI, GFDL, CNRM and ACCESS) for the period 1970 to 2005.

(b). Seasonal mean cycle of maximum temperature data (°C) from IMD (observed data), CRU Reanalysis and Cordex South Asia model data (LMDZ, MPI, GFDL, CNRM and ACCESS) for the period 1970 to 2005.

(c). Seasonal mean cycle of minimum temperature data (°C) from IMD (observed data), CRU reanalysis and Cordex South Asia model data (LMDZ, MPI, GFDL, CNRM and ACCESS) for the period 1970 to 2005.

(Fig. 2b and c); though the simulated magnitudes are much lower than those from the observations.

3.4. Spatial plot of trend analysis JJAS for historical data from 1970 to 2005

In Fig. S6, the trend in the RF-$_{JJAS}$ season for the period 1970 to 2005 from each precipitation dataset used is plotted. The IMD data shows a rising trend from the rest of the datasets. While the RF-$_{JJAS}$ from the IMD exhibits an increasing trend of about 0.5 mm/year in the western NEI and decreasing trend of about 0.6 mm/year in the eastern portion of the NEI, the APHRODITE datasets indicate a weaker but increasing trend in a larger portion of the NEI. All models, in general, qualitatively reproduce the increasing trend in the western NEI, through with weaker magnitudes. The MPI and GFDL models and the ACCESS model somewhat weakly, simulate a negative trend in pockets, which is not seen in observations.

A trend analysis of T$_{Max-JJAS}$ maximum temperature from 1970 to 2005 is plotted in Fig. (S7) where the IMD data shows a positive trend 0.015 °C/year increasing towards the south. The CRU data, on the other hand, shows higher magnitude of trend than the IMD and an increasing trend towards the centre. Models other than the MPI and ACCESS models show a positive trend.

A trend of 0.02 °C/year in the T$_{Min-JJAS}$ is shown from the IMD datasets (Fig. S8), increasing towards the west from the east. On the contrary, the CRU datasets show an increasing trend towards the centre. The LMDZ model shows a higher magnitude of trend than the rest of the datasets, with an increasing trend of 0.05 °C/year. The MPI, GFDL and CNRM models are more or less similar with a lower positive trend in the central portion. The ACCESS model shows an increasing trend towards the north.

3.5. Spatial plot of trend analysis DJF for historical data from 1970 to 2005

Fig. (S9) shows the trends in the observed and simulated RF-$_{DJF}$ in

Table 2

Significance tests using Mann-Kendall and Student *t*-test for maximum temperature data from the IMD, NCEP and climate model data for the period 1970–2005.

Data used	Mann-Kendall test		Student *t*-test			Nature of the trend
	Z value & α value	Statistic value (S)	*p*-Value	t-Value	Trend value	
JJAS						
LMDZ	4.19 > 1.96	308	0.00 < 0.05	5.53 > 2	1.14	Increasing trend & **significant**
GFDL	2.39 > 1.96	176	0.01 < 0.05	2.92 > 2	1.07	Increasing trend & **significant**
ACCESS	2.86 > 1.96	210	0.01 < 0.05	2.61 > 2	1.25	Increasing trend & **significant**
DJF						
LMDZ	3.79 > 1.96	290	0.00 < 0.05	4.52 > 2	2.35	Increasing trend & **significant**
CNRM	2.33 > 1.96	178	0.05 = 0.05	2.02 > 2	1.22	Increasing trend & **significant**
ACCESS	2.22 > 1.96	170	0.02 < 0.05	2.39 > 2	1.28	Increasing trend & **significant**

the NEI for the period 1970 to 2005 where all the datasets show a similar increasing trend in most of the region. The IMD data shows an increasing trend of 0.01 mm/year towards the southwest of the region, and a decreasing trend of 0.4 mm/year towards the north eastern. The Aphrodite data shows a positive trend in most of the regions. Rest of the models except for the LMDZ shows a similar positive trend.

The IMD datasets show an increasing trend in the $T_{Max-DJF}$ from northwest towards the south east; with respective values of 0.03 °C/year and 0.06 °C/year (Fig. S10). CRU datasets shows a higher trend than the IMD datasets. Only the LMDZ model shows a very high positive trend of 0.06 °C/year increasing towards the north. GFDL and CNRM models show an increasing positive trend towards the east while decreasing at central east. MPI model shows an increasing trend in the central portion while the ACCESS model shows a decreasing trend in the central portion. All the datasets show a positive trend.

Fig. (S11) shows the trend analysis of $T_{Min-DJF}$ minimum temperature, from which it is clear that the IMD datasets show an increasing trend of 0.04 °C/year towards the west while CRU data shows a higher trend as compare to the IMD data. Here also, the LMDZ model shows a higher magnitude of trend of 0.07 °C/year increasing towards the north and south while decreasing in the centre. The CNRM and ACCESS models show an increasing trend towards the central east and decreasing trend at the west, opposite to that in the MPI model. The ACCESS model shows an increasing trend in the central east and decreases at the west.

From the above discussion, is it clear that there is some agreement between the IMD and Aphrodite datasets as far as the location of highest and lowest trends in the rainfall, particularly during summer monsoon is concerned. However, the same cannot be told about the agreement between the IMD datasets and CRU datasets in relation to the spatial distribution of the trends in temperature. This is not so surprising given that the CRU datasets are not observational datasets, but model forecasts constrained by the observations. We also note that the models are not up to simulating the spatial distribution of the trends well. As the region is well known for its high convective rainfall associated with complex orography along with relatively high mountains and rainfall processes of the monsoon system, the interpolation and calibration algorithms could contribute to the uncertainty. However, if the historical simulations from various models can at least replicate the area-averaged trends in the climate parameters over the NEI, we can have a qualitative confidence in their future projections. In the next section, we precisely explore this aspect.

3.6. Area-averaged trend analysis from the observations and models for the 1970 to 2005 period

In this section, we report results from the analysis of the area-averaged trends in rainfall and temperature in the NEI region. The significance of these tests was evaluated using both Mann-Kendall and Student's *t*-test. We find that the IMD and Aphrodite datasets show, respectively, increasing and decreasing trends, which are however, not

statistically significant (not shown as all the results show insignificant). Insignificant decreasing or no trend in the summer monsoon precipitation of NEI, as seen from some stations observations in the NEI has been also reported by Jain et al., 2012; Laskar et al., 2014 and Dash et al., 2015. All the model simulations also simulate only insignificant trends.

Further, both IMD and Aphrodite datasets only show a decreasing but statistically insignificant trend in the area averaged rainfall during the DJF (RF_{-DJF}) season in the NEI. The area-averaged trends in the corresponding RF_{-DJF} from various CORDEX models are also seen to be insignificant, though the GFDL and CNRM models show an increasing trend.

Though the nature of trends in the rainfall is insignificant in all the data sets, it indicates a decline in the rainfall over NEI, in tandem with such a signal in the summer monsoon rainfall in rest of India (Krishnan et al., 2016). On longer time scales, the warmer tropical ocean, especially the central eastern Pacific and the western Indian Ocean are suggested to play a role in weakening the monsoon (Roxy et al., 2015).

Only the significant results are shown in the Table 2. The time series of the area-averaged JJAS maximum temperature and that for the DJF season, from the IMD datasets for the period of 1970 to 2005 show an increasing but statistically insignificant trends. Growing population accompanied by massive urbanization, changes in land use, enormous highway development, increases in deforestation, biomass burning, fossil fuel consumption and increasing atmospheric concentrations of greenhouse gases are suspected to be the cause of the changes in temperature (Kothyari and Singh, 1996; Jhajhariaa and Singh, 2011).

Notably, the CRU datasets for both the seasons show an insignificant increasing trend and also, all the models successfully reproduce the observed increasing trends in the area-averaged seasonal maximum temperatures, through most of the simulated trends are statistically significant.

Importantly, we find statistically significant increasing trends in the area-averaged minimum temperature over the NEI during both summer and winter seasons over the period 1970 to 2005 (Table 3). It is intriguing that only the minimum temperature shows a statistically significant increasing trend, while the rainfall trends, though decreasing, are not significant.

From all these results, we can summarize that the downscaled CORDEX South-Asia datasets are successful in capturing the area-averaged seasonal cycles of rainfall and temperature observed during 1970–2005, and are also capable of capturing the corresponding trends, at least qualitatively. However, the climatological spatial distribution and the local long term trends are not well captured, and are also subject to the uncertainties in the observations. Being an orographic region, uncertainty between datasets is largest in North East India (Kulkarni et al., 2013 and Prakash et al., 2014).

3.7. Teleconnections of the historical data (1970–2005) with Nino 3.4

Table S1 shows the teleconnections results ENSO, which is

Table 3

Significance tests using Mann-Kendall and Student *t*-test for minimum temperature data from the IMD and climate model data for the period 1970–2005.

Data used	Mann-Kendall test		Student *t*-test			Nature of the trend
	Z value & α value	Statistic value (S)	*p*-Value	t-Value	Trend value	
JJAS						
IMD	3.26 > 1.96	240	0.00 < 0.05	4.48 > 2	0.63	Increasing trend & **significant**
LMDZ	4.79 > 1.96	352	0.00 < 0.05	7.92 > 2	1.32	Increasing trend & **significant**
MPI	2.48 > 1.96	182	0.03 < 0.05	2.92 > 2	0.61	Increasing trend & **significant**
GFDL	2.04 > 1.96	150	0.03 < 0.05	2.23 > 2	0.66	Increasing trend & **significant**
ACCESS	3.19 > 1.96	234	0.02 < 0.05	2.45 > 2	0.85	Increasing trend & **significant**
DJF						
IMD	3.92 > 1.96	300	0.00 < 0.05	4.59 > 2	1.19	Increasing trend & **significant**
LMDZ	4.15 > 1.96	318	0.00 < 0.05	5.42 > 2	2.97	Increasing trend & **significant**
MPI	3.22 > 1.96	246	0.00 < 0.05	3.24 > 2	1.59	Increasing trend & **significant**
GFDL	2.17 > 1.96	166	0.05 = 0.05	2.99 < 2	0.75	Increasing trend & **significant**
CNRM	2.30 > 1.96	176	0.03 < 0.05	2.33 > 2	1.11	Increasing trend & **significant**
ACCESS	3.16 > 1.96	242	0.00 < 0.05	3.70 > 2	1.62	Increasing trend & **significant**

represented by the well-known NINO3.4 index, with precipitation, maximum and minimum temperature parameters from all relevant the datasets used in this study from the IMD, Aphrodite, CRU and all the models datasets for historical period from 1970 to 2005. The results of this study suggest that the ENSOs do not have any statistically significant impacts on the NEI precipitation and temperature, be it summer or winter, for the period.

3.8. Seasonal mean cycle for simulated future precipitation, maximum and minimum temperature data for the period 2011 to 2060

The individual model RCP4.5 projections of the seasonal cycle of precipitation for the 2011 to 2060 (Fig. 3a) indicate an evolution similar to the corresponding historical cycle. A majority of models, however, indicate a slight decrease or no change in the magnitude of the summer monsoon rainfall, except the projection from the CNRM showing a moderate increase in July precipitation. Based on these results as well as an analysis of the spatial distribution of the simulated precipitation (to be discussed in the next paragraph), we can sum up that the models project slight or no decrease in the rainfall over the NEI in future.

The simulated seasonal cycles of maximum and minimum temperature from the RCP4.5 shows an unchanged evolution, but models also project a substantially increased in the maximum and minimum temperatures (Fig. 3b & c) relative to the corresponding historical simulations which indicates a rise in the temperature in the future over the NEI.

3.9. Simulated JJAS future climatology (RCP4.5) from 2011 to 2060

The simulated JJAS climatology of precipitation (RF-$_{JJAS}$) from the RCP4.5 projections for the 2011–2060 is presented in Fig. (S12), and the excess or deficit as compared to the corresponding historical simulations of is shown in Fig. 1a. We find from Figs. S12 and 4a that the future projection of RF-$_{JJAS}$ from each CORDEX South-Asia model is not significantly different from the corresponding historical simulations (Fig. 1a), except for a weak decrease seen in simulations of a model or two. The RF-$_{JJAS}$ of LMDZ model spatially ranges from 5 to 11 mm while in the rest of the models varies from 3 to 19 mm.

Notably, (the spatial distribution of T$_{Max-JJAS}$ and T$_{Min-JJAS}$) in all the models in Fig. S13 and S14 show an increasing magnitude and are also warmer than the corresponding historical simulations (also match with Fig. 4b and c) across the NEI as compared to the respective historical simulation, with the temperature values ranging from 13 °C to 30 °C and 5 °C to 23 °C for minimum temperature.

3.10. Simulated DJF future climatology (RCP4.5) from 2011 to 2060

The DJF climatology of precipitation (RF-$_{DJF}$) in all the models does not show much change in the future projection (Fig. S15), with values ranging from 0.6 to 3.2 mm, which is also seen in Fig. 5a, though all the models are not simulating the same result, the range of RF-$_{DJF}$ is seen declining in the future projection.

All the models also project an increased T$_{Max-DJF}$ (Figs. S16 and 5b), with the values varying from 2 °C to 17 °C. Spatial distributions of T$_{Max-DJF}$ from the analyzed in all CORDEX South-Asia projections, the models are similar to those from the historical simulations (Fig. S4).

The projected minimum temperatures for DJF season (Figs. S17 and 5c) also increases than the corresponding historical simulations (Fig. S5). The future projected DJF climatology in the NEI range from −10 °C to 8 °C.

3.11. Area-averaged Trends in projected climate in the NEI for the period of 2011 to 2060

Table 4 shows that the JJAS precipitation signals for the 2011 to 2060 period as simulated in the LMDZ and CNRM models show a significantly increasing trend. The ACCESS model projects an increasing but statistically insignificant trend in summer precipitation during the above period. On the other hand, the MPI and GFDL models show an insignificant decreasing trend. The projected DJF precipitation in all the models except the ACCESS model shows an insignificantly decreasing trend. The ACCESS model simulates a weak increasing trend. Only the significant results are shown in the table.

Interestingly, four out of five future simulations project a statistically significant increasing trend in summer maximum temperature (Table 5), while all of them project a statistically significant increasing trend in minimum temperatures (Table 6).

The significant increasing trend in the maximum and minimum trend is also projected for the DJF season (Tables 5 & 6). Thus, is clearly despite the fact that, the projected models do not show quantitatively similar results, qualitatively there is a good agreement, particularly for the temperature. That is, as per the RCP4.5 simulations, the DJF precipitation is expected to further decline while both maximum and minimum temperature are likely to increasing further rapidly. However, there is considerable inter-model uncertainty in the future summer monsoon rainfall in the NEI.

3.12. Extremes analysis for JJAS and DJF seasons for historical and future projections for precipitation, maximum temperature and minimum temperature

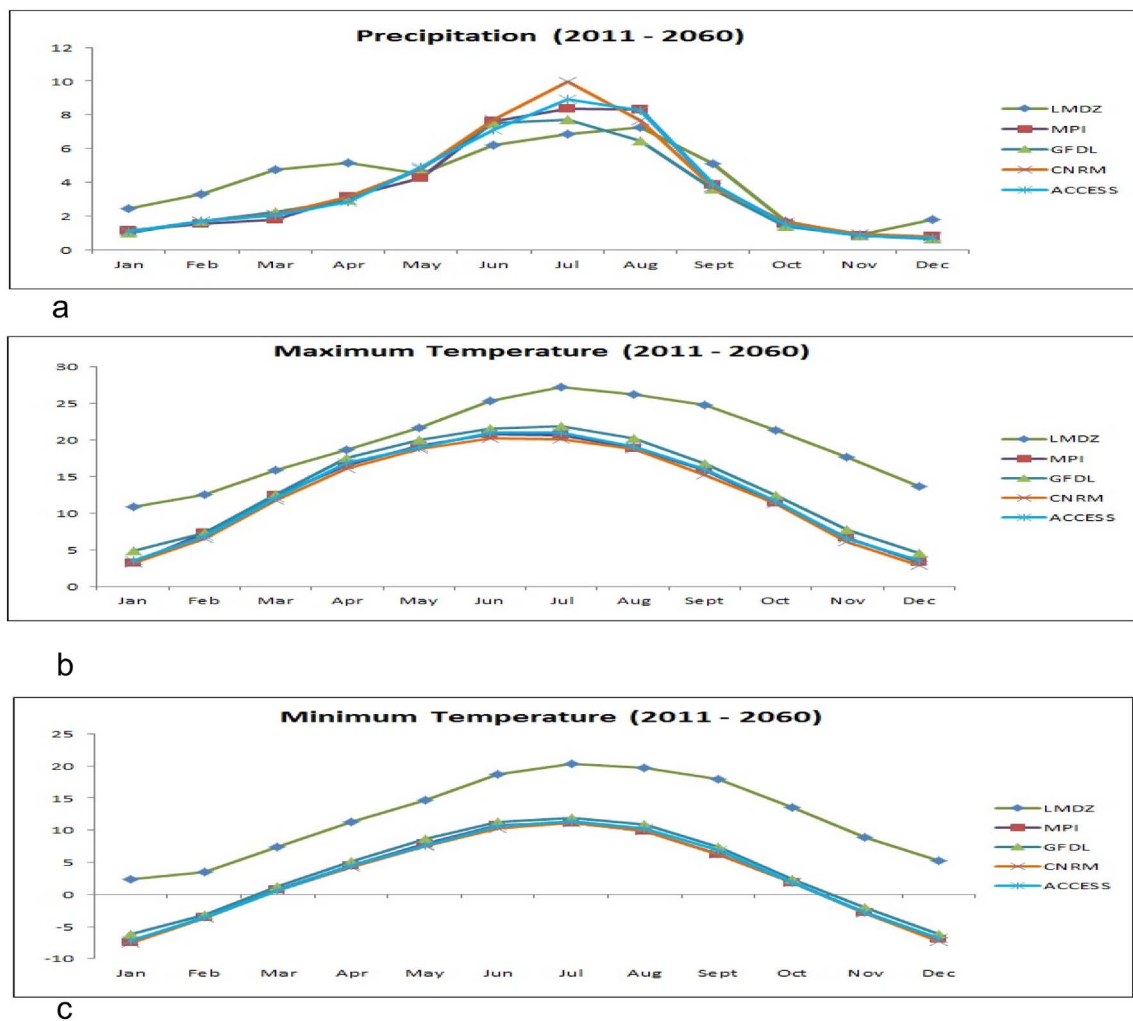In the Fig. 6a & b, histograms of observed and simulated JJAS

Fig. 3. (a). Seasonal mean cycle of precipitation data (mm) from Cordex South Asia model data (LMDZ, MPI, GFDL, CNRM and ACCESS) for the period 2011 to 2060.
(b). Seasonal mean cycle of maximum temperature data (˚C) from Cordex South Asia model data (LMDZ, MPI, GFDL, CNRM and ACCESS) for the period 2011 to 2060.
(c). Seasonal mean cycle of minimum temperature data (˚C) from Cordex South Asia model data (LMDZ, MPI, GFDL, CNRM and ACCESS) for the period 2011 to 2060.

monthly mean rainfall over the NEI for the historical period from 1970 to 2005, and simulated future projections from 2011 to 2060 are presented. While there are four heaviest rainfall monsoon seasons with rainfall of 23 mm/day in NEI as per the IMD datasets, the APHRODITE datasets indicate (Fig. 6a) five heaviest rainfall months with rainfall amounting to 15 mm/day. Except the LMDZ model, all other models simulate the heaviest seasonal rainfall of 15 mm/day, and only two models simulate at least four such extreme rainfall months (Fig. 6a); The LMDZ model simulates only one heaviest rainfall month, with the magnitude of the rainfall amounting to 11 mm/day.

The frequency of the heaviest monthly-mean rainfall months in general increases in the simulated future projections for 2011–60, except in those from the GFDL which fall from 15 to 13 (Fig. 6b). Further, it is also to be noted that the magnitude of the heaviest monthly rainfall decreases (increases) in two (one) models by about 2 mm/day (4 mm/day). Importantly, Fig. 6a and b show that the total number of 'low rainfall' months (arbitrarily defined as rainfall < 7 mm/day) have increased quite substantially, with the range of increase being 34%–42%. It is, however, to be noted that the frequencies of simulated low rainfall event months for the historical period are heavily over-estimated as compared to those from the corresponding IMD frequency.

Histograms of observed and simulated DJF monthly mean rainfall over the NEI for the historical period from 1970 to 2005, and simulated future projections from 2011 to 2060 are presented in the Figs. S18 & S19. The number of heaviest winter monsoon rainfall months is

relatively low as corresponding to the summer monsoon season, as can be seen from both IMD and Aphrodite datasets (Fig. 6a & 6b). The models in general also qualitatively reproduce the difference. However, the heaviest rainfall simulated by the in LMDZ model of 7 mm/day in simulated historical period is noticeably high as compared to the 4.5 mm/day. In future projections, the frequency of simulated heavy rainfall months increases in all the model projections except GFDL and CNRM.

The extreme events of JJAS maximum temperature for the historical period from 1970 to 2005 and for future projections from 2011 to 2060 are shown the Figs. S20 & S21. The observation data from IMD recorded 39 highest maximum temperature months with 34 ˚C/day. The CRU and all the models record somewhat lower maximum temperature than the observation data, ranging from 22 ˚C to 28 ˚C (Fig. S20). The simulated highest maximum monthly temperature in the future projections relatively increases, and ranges between 24 ˚C to 32 ˚C with LMDZ (Fig. S21).

In the Figs. S22 & S23, the extreme months of maximum temperature for DJF season are shown for historical period (1970–2005) and future projections (2011–2060). IMD records show 30 months of the highest monthly maximum temperature of 30 ˚C/day during the historical period. The CRU records show monthly mean highest temperature 27 ˚C/day and all the models show a highly underestimated maximum temperature ranging from 9 ˚C to 15 ˚C. Even though the highest maximum temperature increases in the future projections, the
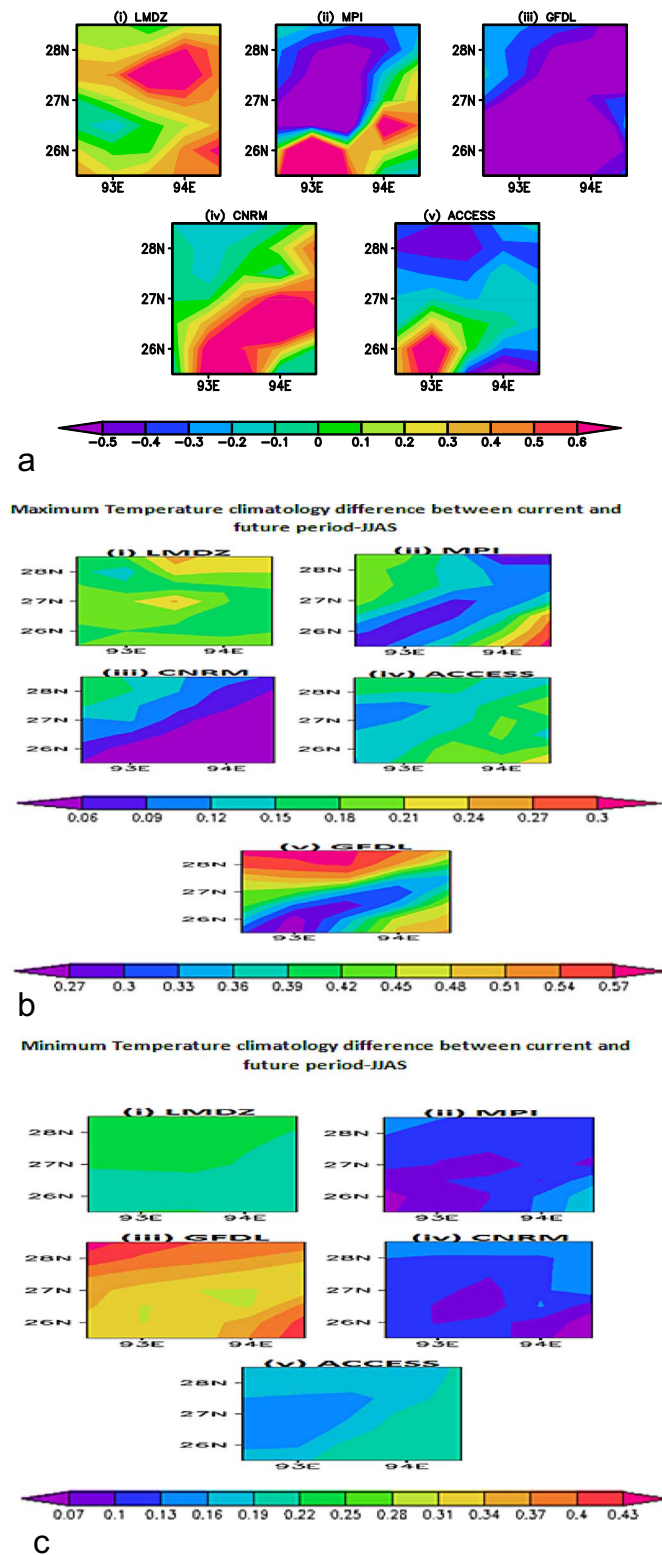
Fig. 4. (a). Climatology difference for precipitation (mm) between current and future period for JJAS for model data, namely, (i) LMDZ, (ii) MPI, (iii) GFDL, (iv) CNRM and (v) ACCESS.
(b). Climatology difference for maximum temperature (°C) between current and future period for JJAS for model data Cordex South Asia: (i) LMDZ, (ii) MPI, (iii) CNRM, (iv) ACCESS and (v) GFDL. Separate color bar has been plotted because of the large difference in the range of climatology in GFDL model.
(c). Climatology difference for minimum temperature (°C) between current and future period for JJAS for model data Cordex South Asia: (i) LMDZ, (ii) MPI, (iii) CNRM, (iv) GFDL and (v) ACCESS.

maximum number of events with highest frequency decreases.

Figs. S24 & S25 show the minimum temperature for JJAS season for historical period (1970–2005) and future projections (2011–2060). The observation data and CRU datasets record a minimum monthly temperature of 27 °C/day. The minimum temperature in all the models is underestimated, with a range of 12 °C to 21 °C across the models. While the simulated frequency of highest minimum temperature in the three future projections increases, only models (LMDZ and GFDL) project a decreasing number of highest minimum temperature events.

In the case of the DJF season, for the historical period (1970–2005), the observation data records minimum temperatures of 16 °C/day and CRU being 26 °C/day. However all the models underestimate the minimum temperature, with a range from 6 °C to −2 °C. The highest minimum temperature in the future projections increases as compared to the corresponding historical simulations.

4. Conclusions

This work studies the climate trends in the northeast India (NEI) using observations during 1970–2005, a period for which five high resolution (50 km) climate simulations, known as historical simulations, are available under the aegis of CORDEX South Asia. The observation datasets we use are gridded data of rainfall and, maximum and minimum temperature from IMD at 1° × 1° resolution (Rajeevan et al., 2005, 2008, 2008), and Aphrodite datasets at 0.5° × 0.5° resolution (Yatagai et al., 2012), along with mean temperature from CRU TS v. 4.00 (0.5° × 0.5° resolution) from 1970 to 2005. Further, using the historical and future climate change projections of the CORDEX South Asia, we estimate the possible future climate change under the RCP4.5 conditions, which is designed to reflect a scenario of moderate anthropogenic emissions from 2011 to 2060. These five regional climate model dataset are generated by the LMDZ, MPI, GFDL, CNRM and ACCESS models.

We find that the seasonal cycle of rainfall and temperature of the NEI are in conformation with that over the rest of the Indian region. There is a reasonable agreement in the area-averaged seasonal cycle and climatology of the rainfall in NEI between the IMD and Aphrodite datasets. However, we find that there are differences in the locations of highest and lowest climatological rainfall and temperatures, maximum trend region, etc. during the summer monsoon. Such a mismatch of location is also seen in the models. Such a discrepancy across the observations/reanalysis and model datasets is seen in the spatial distribution of the maximum and minimum temperatures also. Therefore, one needs to be mindful of this limitation while using these observations and model results in local climate change adaptation planning.

Interestingly, there is a reasonable synergy across the observations and models when the climate signals are area-averaged over the NEI. We find a weak and statistically insignificant decreasing trend in the area-averaged summer monsoon rainfall in the NEI. The IMD observations also show an increasing minimum temperature trend of 0.63 °C and 1.19 °C in 36 years that is statistically significant for both the summer and winter seasons respectively. While the maximum temperatures have also been increasing, the trend is not statistically significant. The area-averaged trends, particularly in the summer monsoon, are in general agreement with those reported in various earlier studies that are based on a few selected stations (Jain et al., 2012; Laskar et al., 2014 and Dash et al., 2015).

Importantly, the area-averaged rainfall and temperatures from the historical simulations also qualitatively reproduce the observed trends, though they overestimate the statistical significance in some instances. This tells us that we can have some confidence in the area-averaged trends in future climate change projections for the NEI. The future projections suggest that there will be a significant increasing trend in the minimum temperature (ranging from 0.71 °C/50 years to 2.6 °C/ 50 years for summer and 1.15 °C/50 years to 2.61 °C/50 years for winter season) and maximum temperature (0.33 °C/50 years to
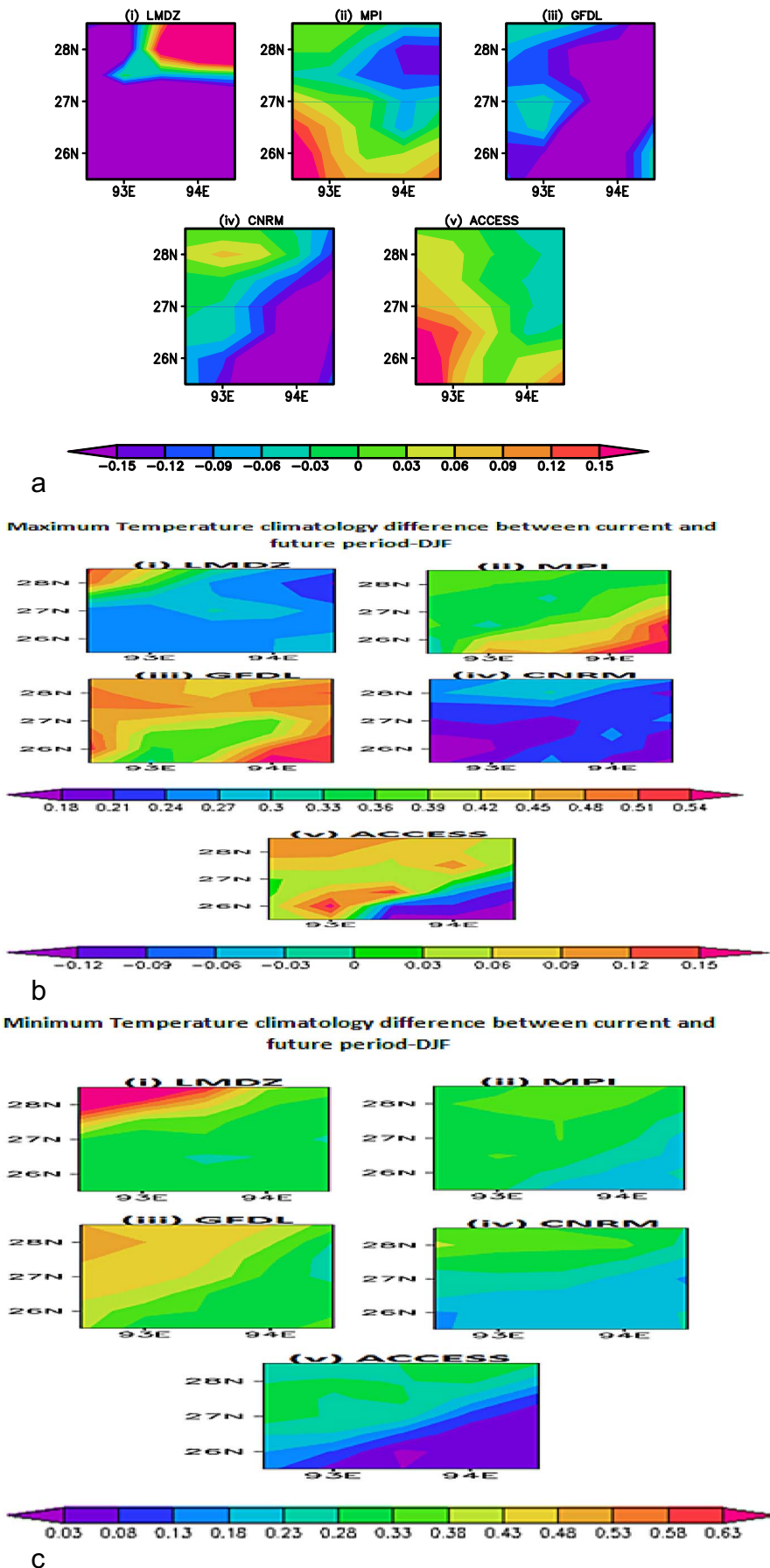
Fig. 5. (a). Climatology difference for precipitation (mm) between current and future period for JJAS for model data Cordex South Asia: (i) LMDZ, (ii) MPI, (iii) GFDL, (iv) CNRM and (v) ACCESS.

(b). Climatology difference for maximum temperature (°C) between current and future period for DJF for model data Cordex South Asia: (i) LMDZ, (ii) MPI, (iii) CNRM, (iv) GFDL and (v) ACCESS. Separate color bar has been plotted because of the large difference in the range of climatology in ACCESS model.

(c). Climatology difference for minimum temperature (°C) between current and future period for DJF for model data Cordex South Asia: (i) LMDZ, (ii) MPI, (iii) CNRM, (iv) GFDL and (v) ACCESS.

Table 4
Significance tests using Mann-Kendall and Student *t*-test for precipitation data from the climate model data for the period 2011–2060.

Mann-Kendall test			Student *t*-test			
Data used	Z value & α value	Statistic value (S)	*p*-Value	t-Value	Trend value	Nature of the trend
LMDZ	3.17 > 1.96	379	0.00 < 0.05	3.10 > 2	0.67	Increasing trend & **significant**
CNRM	1.97 > 1.96	235	0.04 < 0.05	2.07 > 2	1.08	Increasing trend & **significant**

Table 5
Significance tests using Mann-Kendall and Student *t*-test for maximum temperature data from the climate model data for the period 2011–2060.

Data used	Mann-Kendall test		Student *t*-test			Nature of the trend
	Z value & α value	Statistic value (S)	*p*-Value	t-Value	Trend value	
JJAS						
LMDZ	5.73 > 1.96	685	0.00 < 0.05	7.01 > 2	1.4	Increasing trend & **significant**
MPI	3.29 > 1.96	393	0.00 < 0.05	4.24 > 2	1.13	Increasing trend & **significant**
GFDL	6.25 > 1.96	747	0.00 < 0.05	8.84 > 2	2.86	Increasing trend & **significant**
ACCESS	3.81 > 1.96	455	0.00 < 0.05	4.07 > 2	1.07	Increasing trend & **significant**
DJF						
LMDZ	4.47 > 1.96	551	0.00 < 0.05	5.24 > 2	1.96	Increasing trend & **significant**
MPI	3.63 > 1.96	447	0.00 < 0.05	4.27 > 2	2.71	Increasing trend & **significant**
GFDL	4.41 > 1.96	543	0.00 < 0.05	4.84 > 2	3.01	Increasing trend & **significant**
CNRM	3.27 > 1.96	403	0.00 < 0.05	7.19 > 2	1.89	Increasing trend & **significant**

Table 6
Significance tests using Mann-Kendall and Student *t*-test for minimum temperature data from the climate model data for the period 2011–2060.

Data used	Mann-Kendall test		Student *t*-test			Nature of the trend
	Z value & α value	Statistic value (S)	*p*-Value	t-Value	Trend value	
JJAS						
LMDZ	7.25 > 1.96	867	0.00 < 0.05	11.78 > 2	1.66	Increasing trend & **significant**
MPI	3.89 > 1.96	465	0.00 < 0.05	4.27 > 2	0.95	Increasing trend & **significant**
GFDL	6.92 > 1.96	827	0.00 < 0.05	10.44 > 2	2.6	Increasing trend & **significant**
CNRM	2.68 > 1.96	321	0.01 > 0.05	2.87 > 2	0.71	Increasing trend & **significant**
ACCESS	5.08 > 1.96	607	0.00 < 0.05	6.20 > 2	1.45	Increasing trend & **significant**
DJF						
LMDZ	5.03 > 1.96	619	0.00 < 0.05	6.47 > 2	2.61	Increasing trend & **significant**
MPI	4.96 > 1.96	611	0.00 < 0.05	5.23 > 2	1.94	Increasing trend & **significant**
GFDL	4.64 > 1.96	571	0.00 < 0.05	6.07 > 2	2.38	Increasing trend & **significant**
CNRM	5.71 > 1.96	703	0.00 < 0.05	7.19 > 2	1.89	Increasing trend & **significant**
ACCESS	2.89 > 1.96	357	0.00 < 0.05	3.08 > 2	1.15	Increasing trend & **significant**

2.86 °C/50 years for summer & 0.87 °C/50 years to 3.01 °C/50 years for winter season), and a possible decreasing but statistically insignificant trend in summer and winter rainfall in the NEI for the 2011–2060 period. In summary, notwithstanding the uncertainties, when the NEI is taken as a whole, as the models qualitatively capture the historical trend, we can conjecture, that the future projections of decrease in rainfall and increase in temperature may be expected to be realized, though quantifying the same would be difficult. We also find that the ENSO events do not have any significant impact on the climate of the NEI, and, we may not expect any perceivable impact of ENSOs.

Extreme monthly means for precipitation and maximum and minimum temperature for historical and future projections have also been studied over NEI for both JJAS and DJF seasons. The simulated models underestimate the extreme mean monthly values. Overall the extreme monthly means of maximum and minimum temperature increase in the future projections. The frequency of simulated the heaviest rainfall months during JJAS increase in the simulated future projections for 2011–60 from four out of five models as compared to the historical period. Having said that, the magnitude of the heaviest monthly rainfall moderately decreases in future projections in two models. Importantly, total number of 'low rainfall' months (arbitrarily defined as rainfall < 7 mm/day) has increased quite substantially, with the range of increase being 34%–42%. All this suggest that the CORDEX models are not definitive about any increase of extreme rainfall months over northeast India during summer monsoon season.

As the region is well known for its high convective rainfall associated with complex orography along with relatively high mountains and rainfall processes of the monsoon system, the interpolation and calibration algorithms could contribute to the uncertainty. To improve the uncertainties in the climatological datasets pertaining to the in NEI, a higher density of observations would be critical to address various sub-regional climate change/variability issues with confidence.
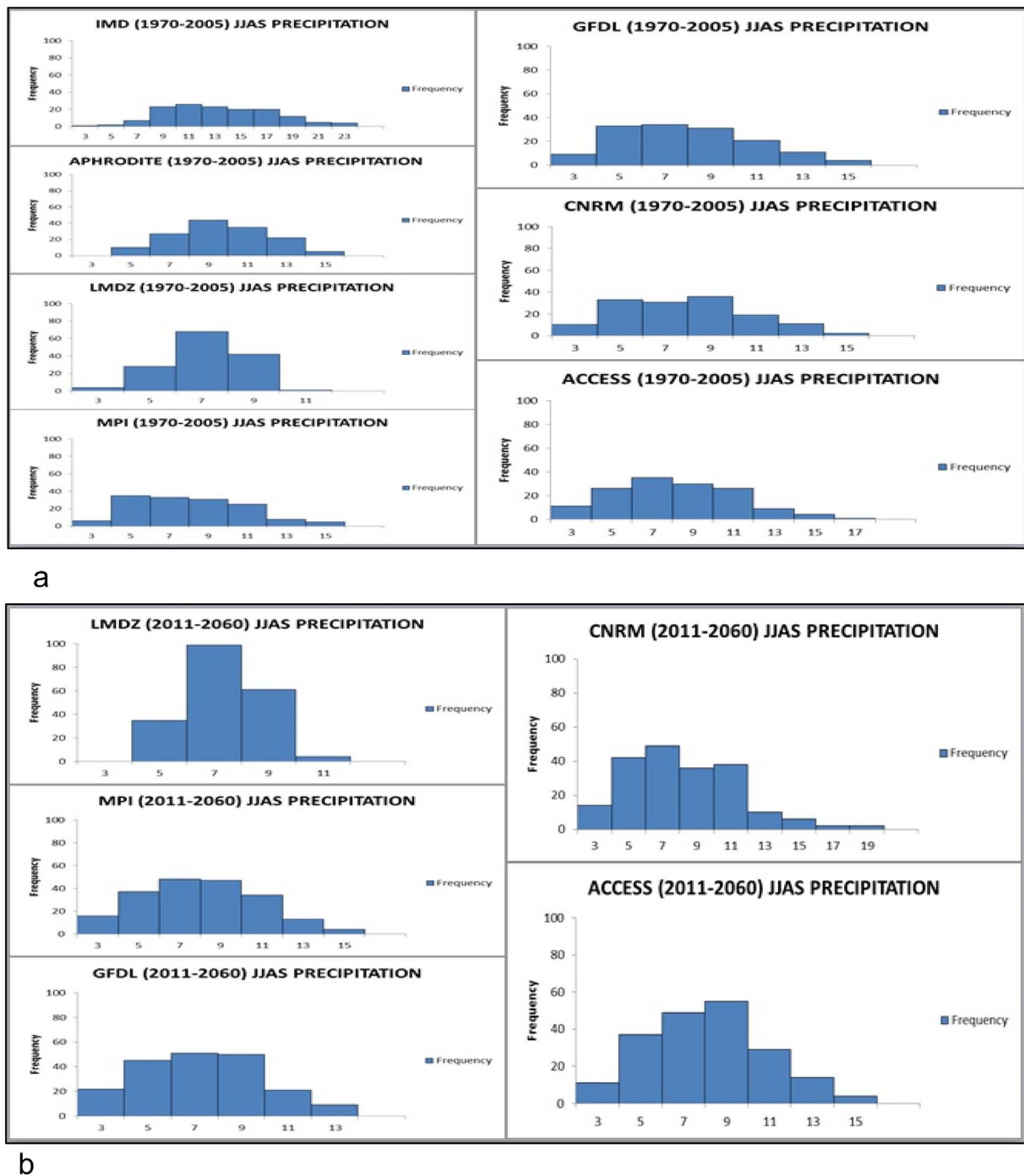
a

b

Fig. 6. (a). Histogram plots for JJAS precipitation (mm) of historical period (1970–2005): IMD, Aphrodite along with CORDEX models ((LMDZ, MPI, GFDL, CNRM and ACCESS).
(b). Histogram plots for JJAS precipitation (mm) of future projections (2011–2060) of CORDEX models ((LMDZ, MPI, GFDL, CNRM and ACCESS).

Appendix 1

The driving simulations of the LMDZ, MPI, GFDL, CNRM and ACCESS are performed within the framework of CMIP5. To downscale the CMIP5 (Coupled Model Intercomparison Project Phase 5) scenarios, the World Climate Research Program (WCRP) initiated a coordinated effort known as CORDEX, which provides an ensemble of high resolution regional climate projections for all the major continental regions of the world. Currently CORDEX involves > 20 RCM groups around the world and provides a quality-controlled data set of downscaled information for historical past and 21st century projections (Taylor et al., 2012). The CORDEX outputs are used for input or adaptation work, and

also for IPCC Fifth Assessment Report (Giorgi et al., 2009). CORDEX focus on the emission scenarios known as RCP4.5 and RCP8.5 which represent a mid and a high level emission scenario, also roughly corresponding to the IPCC SRES emission scenarios B1 and A1B, respectively (Giorgi et al., 2009). These high resolution regional climate models are selected because these models provide an opportunity to dynamically downscale global model simulations to superimpose the regional detail of specific regions and moreover global climate model suffers from errors due to inadequate representation as well as its expensiveness (Krishna Kumar et al., 2011 and Kumar et al., 2006).

Supplementary data

Supplementary data to this article can be found online at https://doi.org/10.1016/j.gloplacha.2017.11.010.

References

Arora, M., Goel, N.K., Singh, P., 2005. Evaluation of temperature trends over India. Hydrol. Sci. J. 50 (1), 81–93.

Chakraborty, R., Deb, B., Devannac, N., Sena, S., 2012. North-East India an ethnic storehouse of unexplored medicinal plants. J. Nat. Prod. Plant Resour. 2 (1), 143–152.

Chaturvedi, R.K., Ravindranth, N.H., Mathangi, J., Jaideep, J., Bala, G., 2012. Multi-model climate change projections for India under representative concentration pathways. Curr. Sci. 103 (7).

Chinchorkar, S.S., Sayad, F.G., Vaidya, V.B., Pandye, V., 2015. Trend detection in annual maximum temperature and precipitation using the Mann Kendal test – a case study to assess climate change on Anand of central Gujarat. Mausam 66 (1), 1–6.

Choudhury, B.U., Das, A., Ngachan, S.V., Slong, A., Bordoloi, L.J., Chowdhury, P., 2012. Trend analysis of long term weather variables in mid altitude Meghalaya, North-East India. J. Agr. Phys. 12 (1), 12–22.

Collins, M., Rao, K.A., Ashok, K., Bhandari, S., Ashis, K., Prakash, M.S., Srivastava, R., Turner, A., 2013. Observational challenges in evaluating climate models. Nat. Clim. Chang. 3, 940–941.

Dash, S.K., Hunt, J.C.R., 2007. Variability of climate change in India. Curr. Sci. 93 (6), 782–788.

Dash, S.K., Sharma, N., Pattnayak, K.C., Gao, X.J., Shi, Y., 2012. Temperature and precipitation changes in the north-east India and their future projections. Glob. Planet. Chang. 98-99, 31–44.

Dash, et al., 2015. Projected seasonal mean summer monsoon over India and adjoining regions for the twenty-first century. Theor. Appl. Climatol. 122, 581–593.

Dubey, D.P., Krishnakumar, G., 2014. Trends in precipitation extremes over Central India. Mausam 65 (1), 103–108.

Dufresne, J.L., Foujol, M.A., Denvil, S., et al., 2013. Climate change projections using the IPSL-CM5 Earth System Model: from CMIP3 to CMIP5. Clim. Dyn. 40, 2123–2165. http://dx.doi.org/10.1007/s00382-012-1636-1.

Giorgi, F., Jones, C., Asrar, G.R., 2009. Addressing climate information needs at the regional level: the CORDEX framework. WMO Bull. 58 (3), 175–183.

Guhathakurta, P., Rajeevan, M., 2008. Trends in the rainfall pattern over India. Int. J. Climatol. 28, 1453–1469. http://dx.doi.org/10.1002/joc.1640.

Harris, P.D., Jones, T.J., Osborna, Listera, D.H., 2014. Updated high-resolution grids of monthly climatic observations – the CRU TS3.10 Dataset. Int. J. Climatol. 34, 623–642.

IPCC, 2007. Climate change 2007: impacts, adaptation and vulnerability. In: Parry, M.L., Canziani, O.F., Palutikof, J.P., van der Linden, P.J., Hanson, C.E. (Eds.), Contribution of Working Group II to the Fourth Assessment Report of the Intergovernmental Panel on Climate Change. Cambridge University Press, Cambridge, UK, pp. 469–506.

IPCC, 2013. Climate change 2013: the physical science basis. In: Stocker, T.F., Qin, D., Plattner, G.-K., Tignor, M., Allen, S.K., Boschung, J., Nauels, A., Xia, Y., Bex, V., Midgley, P.M. (Eds.), Contribution of Working Group I to the Fifth Assessment Report of the Intergovernmental Panel on Climate Change. Cambridge University Press, Cambridge, United Kingdom and New York, NY, USA (1535 pp).

Jain, S.K., Kumar, V., 2012. Trend analysis of rainfall and temperature data for India. Curr. Sci. 102 (1), 37–49.

Jain, S.K., Kumar, V., Saharia, M., 2012. Analysis of rainfall and temperature trends in northeast India. Int. J. Climatol. http://dx.doi.org/10.1002/joc.3483.

Jhajhariaa, D., Singh, V.P., 2011. Trends in temperature, diurnal temperature range and sunshine duration in Northeast India. Int. J. Climatol. 31, 1353–1367.

Jourdain, N.C., et al., 2013. The Indo-Australian monsoon and its relationship to ENSO and IOD in reanalysis data and the CMIP3/CMIP5 simulations. Clim. Dyn. 41, 3073–3102. http://dx.doi.org/10.1007/s00382-013-1676-1.

Kothawale, D.R., Kumar, K.K., Srinivasan, G., 2012. Spatial asymmetry of temperature trends over India and possible role of aerosols. Theor. Appl. Climatol. 110, 263–280. http://dx.doi.org/10.1007/s00704-012-0628-8.

Kothawale, D.R., Kumar, R.K., 2005. On the recent changes in surface temperature trends over India. Geophys. Res. Lett. 32, L18714. http://dx.doi.org/10.1029/2005GL023528.

Kothyari, U.C., Singh, V.P., 1996. Rainfall and temperature trends in India. Hydrol. Process. 10, 357–372.

Krishnan, et al., 2016. Deciphering the desiccation trend of the South Asian monsoon hydroclimate in a warming world. Clim. Dyn. http://dx.doi.org/10.1007/s00382-015-2886-5.

Kulkarni, et al., 2013. Projected climate change in the Hindu Kush–Himalayan region by using the high-resolution regional climate model PRECIS. Mt. Res. Dev. 33 (2), 142–151.

Kumar, K.K., Patwardhan, S.K., Kulkarni, A., Kamala, K., Rao, K.K., Jones, R., 2011. Simulated projections for summer monsoon climate over India by a high-resolution regional climate model (PRECIS). Curr. Sci. 101 (3), 312–326.

Kumar, P., et al., 2013. Downscaled climate change projections with uncertainty assessment over India using a high resolution multi-model approach. Sci. Total Environ. http://dx.doi.org/10.1016/j.scitotenv.2013.01.051.

Kumar, R.K., et al., 2006. High-resolution climate change scenarios for India for the 21st century. Curr. Sci. 90 (3), 334–345.

Kumar, V., Jain, S.K., Singh, Y., 2010. Analysis of long-term rainfall trends in India. Hydrol. Sci. J. 55 (4), 484–496.

Laskar, S.I., Kotal, S.D., Roy, S.K.B., 2014. Analysis of rainfall and temperature trends of selected stations over Northeast India during last century. Mausam 65 (4), 497–508.

Mondal, A., Khare, D., Kundu, S., 2014. Spatial and temporal analysis of rainfall and temperature trend of India. Theor. Appl. Climatol. http://dx.doi.org/10.1007/s00704-014-1283-z.

Mooley, D.A., Parthasarathy, B., 1983a. Variability of the Indian Summer monsoon and tropical circulation features. Am. Meteorol. Soc. 111 (5), 967–978.

Mooley, D.A., Parthasarathy, B., 1983b. Indian Summer Monsoon and E1 Nino. Pure Appl. Geophys. 121 (2), 339–352.

Pant, G.B., Kumar, R.K., 1997. Climates of South Asia. (ISBN: 978-0-471-94948-0).

Parthasarathy, B., Rupakumar, K., Munot, A.A., 1996. Homogeneous regional summer monsoon rainfall over India: inter annual variability and teleconnections. Res. Rep (RR–070, ISSN, 0252–1075).

Prakash, S., et al., 2014. Seasonal intercomparison of observational rainfall datasets over India during the southwest monsoon season. Int. J. Climatol. http://dx.doi.org/10.1002/joc.4129.

Rajeevan, M., Bhate, J., Jaswal, A.K., 2008. Analysis of variability, and trends of extreme rainfall events over India using 104 years of gridded daily rainfall data. Geophys. Res. Lett. 35, L18707. http://dx.doi.org/10.1029/2008GL035143. (…..august).

Rajeevan, M., Bhate, J., Kale, J.D., Lal, B., 2005. Development of a high resolution daily gridded rainfall data for the Indian region. IMD Met Monograph No: Climatology 22/2005. pp. 27 (Available from National Climate Centre, IMD Pune. ncc@imdpune.gov.in).

Rajeevan, M., Srivastava, A.K., Kshirsagar, S.R., 2008. Development of a high resolution daily gridded temperature data set (1969–2005) for the Indian Region. In: NCC Research Report 8. National Climate Centre India Meteorological Department.

Rajendran, K., Sajani, S., Jayasankar, C.B., Kitoh, A., 2013. How dependent is climate change projection of Indian summer monsoon rainfall and extreme events on model resolution? Curr. Sci. 104 (10), 1409–1418.

Ravindranath, et al., 2011. Climate change vulnerability profiles for North East India. Curr. Sci. 101 (3), 384–394.

Revadekar, J.V., Kothawale, D.R., Patwardhan, S.K., Pant, G.B., Kumar, R.K., 2012. About the observed and future changes in temperature extremes over India. Nat. Hazards 60, 1133–1155. http://dx.doi.org/10.1007/s11069-011-9895-4.

Roxy, M., Kapoor, R., Pascal, T., Murtugudde, R., Ashok, K., Goswami, B.N., 2015. Drying of Indian subcontinent by rapid Indian Ocean warming and a weakening land-sea thermal gradient. Nat. Commun. http://dx.doi.org/10.1038/ncomms8423.

Sabin, T.P., Krishnan, R., Ghattas, J., Denvil, S., Dufresne, J.-L., Hourdin, F., Pascal, T., 2013. High resolution simulation of the South Asian monsoon using a variable resolution global climate model. Clim. Dyn. http://dx.doi.org/10.1007/s00382-012-1658-8.

Saha, A.S., Ghosh, A.S., Sahana, Rao, E.P., 2014. Failure of CMIP5 climate models in simulating post-1950 decreasing trend of Indian monsoon. Geophys. Res. Lett. 41, 7323–7330. http://dx.doi.org/10.1002/2014GL061573.

Sharmila, S., Joseph, S., Sahai, A.K., Abhilash, S., Chattopadhyay, R., 2015. Future projection of Indian summer monsoon variability under climate change scenario: an assessment from CMIP5 climate models. Glob. Planet. Chang. 124, 62–78.

Shashikanth, K., Salvi, K., Ghosh, S., Rajendran, K., 2013. Do CMIP5 simulations of Indian summer monsoon rainfall differ from those of CMIP3? Atmos. Sci. Lett. 15, 79–85. http://dx.doi.org/10.1002/asl2.466.

Taylor, K.E., Stouffer, R.J., Meehl, G.A., 2012. An overview of CMIP5 and the experiment design. Am. Meteorol. Soc. http://dx.doi.org/10.1175/BAMS-D-11-00094.1.

Wagholikar, N.K., Ray, S.K.C., Sen, P.N., Kumar, P.P., 2014. Trends in seasonal temperatures over the Indian Region. J. Earth Syst. Sci. 123 (4), 673–687.

Yatagai, A., et al., 2012. APHRODITE: constructing a long-term daily gridded precipitation dataset for Asia based on a dense network of rain gauges. Am. Meteorol. Soc. http://dx.doi.org/10.1175/BAMS-D-11-00122.1.